



An Investigation of Pulsatile Blood Flow in An Angulated Neck of Abdominal Aortic Aneurysm Using Computational Fluid Dynamics

Open
Access

Yousif A. Algabri¹, Surapong Chatpun^{1,*}, Ishkrizat Taib²

¹ Institute of Biomedical Engineering, Faculty of Medicine, Prince of Songkla University, Hat Yai 90110, Songkhla, Thailand

² Flow Simulation and Turbulence Focus Group, Faculty of Mechanical and Manufacturing Engineering, Universiti Tun Hussein Onn Malaysia, Batu Pahat 86400, Johor, Malaysia

ARTICLE INFO

Article history:

Received 1 February 2019

Received in revised form 18 April 2019

Accepted 2 May 2019

Available online 17 May 2019

ABSTRACT

Hemodynamics in highly proximal neck of abdominal aortic aneurysm (AAA) was investigated in an idealized case by using computational fluid dynamics (CFD) technique. The steady and pulsatile flow simulations were carried out and compared. The three-dimensional model was constructed using CAD software and boundary conditions were adopted from the literature based on experimental studies. Grid independency study was performed to test the computational mesh used. Blood was considered as incompressible and Newtonian fluid in steady and transient regimes with no-slip and rigid aortic wall. Finite volume method based on ANSYS Fluent was used to solve the CFD governing equations. The results acquired from CFD post-processing for velocity distributions and flow rate during steady and transient ($t = 0.25$ s and $t = 0.55$ s) flow states. Furthermore, velocity distributions showed significant differences between the two cases (steady and transient) in the idealized angulated neck AAA model. During the steady state, the flow was concentrated in the middle of aorta while in transient (a systolic phase) the flow was more pronounced and distributed near the wall and tortuous areas more than in a diastolic phase. Flow rate at iliac artery outlets showed different values in both states and slight variance in the right and left iliac arteries. The steady and pulsatile flow comparison using CFD were crucial to understand and investigate the hemodynamic in angulated neck of abdominal aortic aneurysm model.

Keywords:

Hemodynamics; Abdominal aortic aneurysm; CFD; Grid independency; Velocity distributions

Copyright © 2019 PENERBIT AKADEMIA BARU - All rights reserved

1. Introduction

An aneurysm is an abnormal localised enlargement of a part of artery. This morphological abnormality is occurred when the aortic wall becomes vulnerable and weak. It is generally a non-symptomatic disease [1,2]. Yearly, there are more than 15,000 cases of death in the United States from the rupture or dissection of abdominal or thoracic aortic aneurysm [1]. The major reason for

* Corresponding author.

E-mail address: surapong.c@psu.ac.th (Surapong Chatpun)

the formation of abdominal aortic aneurysm (AAA) is associated with so-called Marfan's Syndrome or Ehlers Danlos Syndrome along with risk factors such as hypertension, smoking, age and atherosclerosis [3,4]. If aneurysm is kept untreated, it tends to grow at a rate of 0.08 cm/year and might be ruptured if the diameter of aneurysm reaches 6 cm or larger [5]. The conventional procedure of aneurysm treatment is an open surgery, however, in recent years more non-invasive methods have been introduced including stent grafts and endovascular sealings [6,7].

From biomechanical points of view, the rupture of aneurysm perhaps thought as the failure of material. The traditional determinant of rupture is the maximum diameter of lumen, but it has been found inadequate in several cases. Therefore, determining and understanding the actual rupture's factors clinically are still uncertain. Therefore, to ensure a proper biomechanical analysis for the risk of rupture, hemodynamics and stress state at the lesion and weak wall should be taken into account. Since blood flow exerts both regular and shear forces on the inner wall surface of artery, then those forces can influence the condition of artery wall [8]. Vasava *et al.*, [9] reported that the complex anatomic structures of arteries are mostly influenced by abnormal flow dynamics and distribution of stress, while Dabagh *et al.*, [10] and Towfiq *et al.*, [11] studies have illustrated that the change of aorta size is due to blood pressure.

The recent advanced imaging technologies have been extensively used in cardiovascular system for the visualization of blood flow and demonstration of the flow patterns in order to unveil the pathophysiology of the circulatory system. Computational fluid dynamics (CFD) has proven to be an effective tool and made the simulations of complex systems in industry and academic research feasible [12-14]. CFD plays a significant standard method for the visualization and the analysis of flow in different cases such as blood in arteries, as well as the wall shear stress [15, 16]. Few studies reported that more than 35% of AAA's patients were ineligible for endovascular treatments due to the complexity of AAA morphology such as aortic angulation and proximal short neck of aneurysm [17-19]. Moreover, to measure all the hemodynamic parameters in living human-beings accurately is very difficult because of the cardiac cycles which cause a natural pulsatile flow [20]. Therefore, for these reasons, it is difficult to do *in vivo* experiments. To overcome this challenge, it is beneficial to simulate blood flow through a computational modelling.

In this study, we have constructed a three-dimensional (3D) angulated neck AAA model which adopted from the literature. The idealized aorta model consists of proximal angular neck, aneurysm sac and iliac bifurcations arteries. The steady and pulsatile flows of blood through the 3D angulated neck AAA model with incompressible Navier-Stokes equations were simulated. The boundary conditions along with governing equations are solved by the finite volume method (FVM) in ANSYS Workbench V19.1. Due to the crucial effect of hemodynamic change, geometry's curvature of AAA and flow rate in arteries, the blood flow through proximal neck and aneurysm sac is studied.

Therefore, the velocity flow across different cross-sections for steady and unsteady conditions within angulated neck AAA model are investigated. In this present work, we also investigated the variances between steady and transient flow conditions through idealized and highly angulated neck abdominal artery aneurysm with rigid walls using CFD tools.

2. Methodology

2.1 Geometry

The geometry used in this study was built using a CAD software (Siemens NX 11, Texas, USA). The construction of geometry was a resembling of a fusiform shape of angulated neck of AAA. The geometry was designed with 20 mm inlet, 55 mm aneurysm sac and 11 mm and 10 mm for both outlet iliac arteries as well as the lengths are shown in Figure 1. The angle of the proximal neck was

selected to be 80°, representing a severe neck angulation of abdominal aorta as reported by Hobo *et al.*, [21] that a proximal neck angle greater than 60° is considered to be risky for endovascular repair.

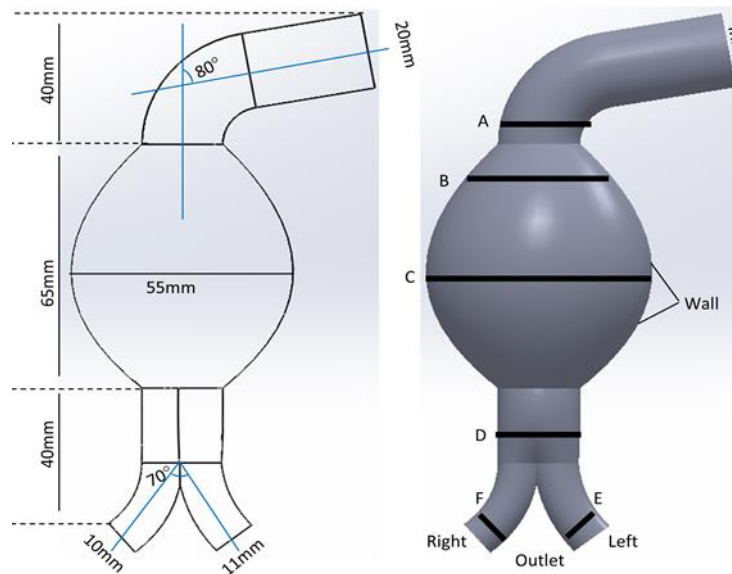


Fig. 1. 3D model of severe angulated neck of idealized AAA. Six selected planes are indicated by black lines (A-F). A and B are upper and lower neck sections, C is mid-sac section and D to F are Iliac bifurcation sections

2.2 Grid and Simulation Design

The computational mesh for the geometry was carried out using ANSYS Workbench v19.1 (ANSYS Inc., Canonsburg, USA). The meshes were generated using tetrahedral cells with five boundary layers of total thickness of 0.2 mm. In order to achieve an optimal mesh, the grid independency study was performed for five different numbers of elements as presented in Table 1. Smoothing and quality checks were carried out to satisfy the refinement of the elements as presented in Figure 2. In this CFD simulation, ANSYS was employed to simulate the blood flow behavior in the angulated neck of idealized AAA. 3D finite volume method was implemented to solve Navier-stokes equations of momentum conservation and continuity for incompressible and Newtonian fluid [22]. These equations are expressed as Eq. (1) and Eq. (2).

$$\rho \left(\frac{\partial u}{\partial t} \right) + \rho (u \cdot \nabla) u = -\nabla P + \mu \nabla^2 u \quad (1)$$

$$\frac{\partial \rho}{\partial t} + \nabla \cdot (\rho u) = 0 \quad (2)$$

where u , P and ∇ denote velocity vector, pressure, and divergence, while ρ and μ for density and dynamic viscosity of fluid.

Table 1
 Number of elements used for
 grid independency test

Mesh	Elements No
Case 1	55,304
Case 2	71,379
Case 3	391,306
Case 4	972,832
Case 5	1,029,702

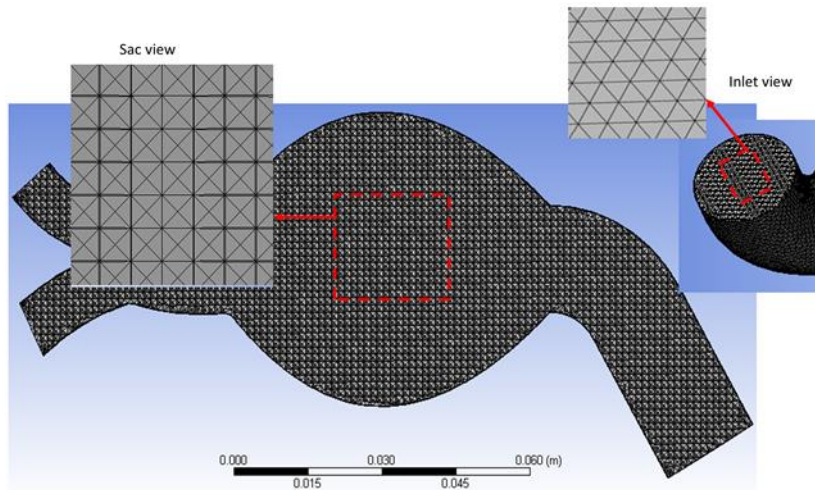


Fig. 2. Mesh view of computational idealized AAA model

2.3 Assumptions and Boundary Conditions

The CFD simulations were performed under steady and transient conditions. Blood was assumed to be laminar, incompressible and Newtonian fluid with a dynamic viscosity of 0.0035 Pa·s at 45% haematocrit and a density of 1,060 kg/m³ [14,23]. For steady-state simulation; the velocity of 0.28 m/s was used for the inlet velocity and outlet pressure of zero. In contrast, for pulsatile simulation; a user-defined function (UDF) code for time-dependent velocity and pressure waveforms were imposed at the inlet and outlet boundaries. Both waveforms were adopted from the experimental study of Olufsen *et al.*, [24] for an abdominal aorta region as shown in Figure 3. The artery wall was assumed as rigid and no-slip condition in both cases.

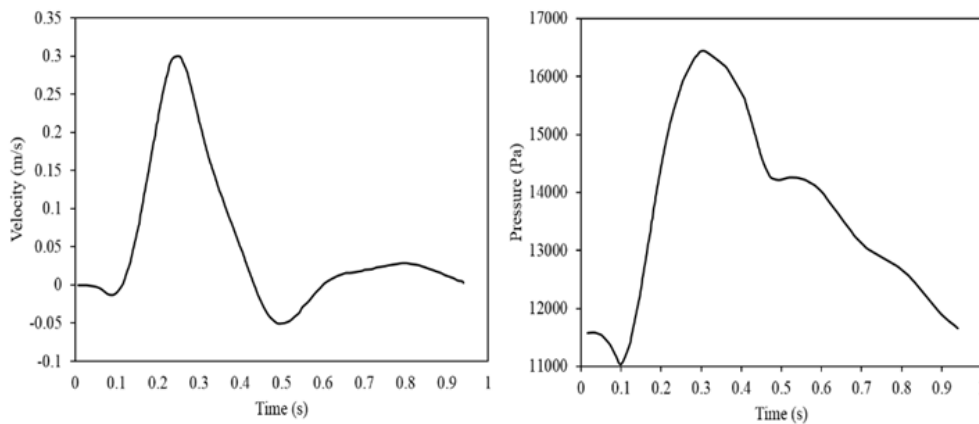


Fig. 3. Inlet velocity and outlet pressure waveforms applied for a pulsatile simulation

2.3 Computation

CFD simulations were carried out using commercial finite volume solver, ANSYS FLUENT CFD v19.1 (ANSYS Inc., Canonsburg, PA, USA). Pressure was calculated by pressure-velocity coupling method using a SIMPLE algorithm. A 2nd order upwind with a pressure-based solver was used for the momentum spatial discretization. Convergence criteria was assigned to 10^{-5} for velocity and continuity residuals [25]. For transient simulation, the calculation was fixed to 0.01 s with 282 iterations for each time-step.

3. Results and discussion

3.1 Mesh Independency Study

The purpose of this sub-study is to obtain the minimal cell size of tetrahedrons for a grid independency flow simulation. The maximum velocity obtained from the five meshes simulations was shown in Figure 4. The plot shows that when elements increase the maximum velocity becomes higher. For the case 4 (972,832 elements) and case 5 (1,029,702 elements), the velocity trends show to be similar. Therefore, the mesh with 972,832 elements was used in this computational study.

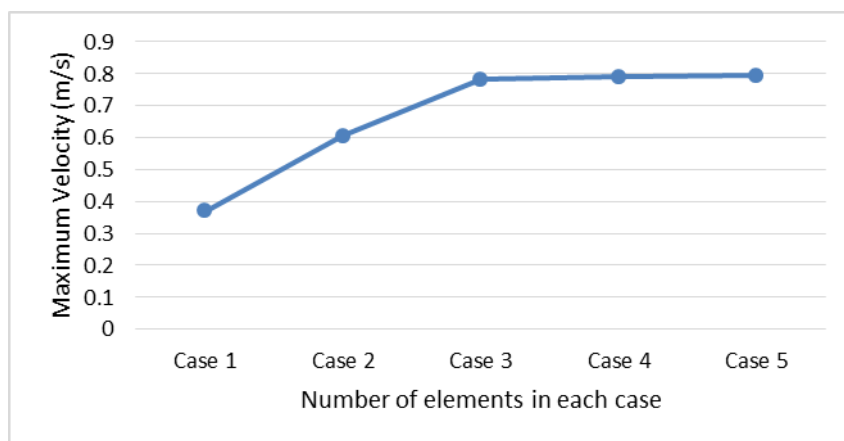


Fig. 4. Grid independency study based on velocity profile

3.2 Velocity Distributions

For better understanding of the expected flow behaviors in an angulated neck AAA, the analysis of solutions to steady and transient conditions using velocity and pressure waveforms are calculated and visualized. For pulsatile flow analysis, the velocity contours were obtained at 0.25 s (peak systole), 0.55 s (early diastole) of a cardiac cycle. In order to obtain the details of velocity flow through the proximal neck, aneurysm sac and bifurcations arteries, velocity profile across six different cross-sectional regions were captured. These regions are (A) neck angle, (B) proximal aneurysm, (C) middle of aneurysm sac, (D) bifurcation arteries and iliac artery outlets (E and F) as illustrated in Figure 5. The axial velocity profiles for steady simulation are presented in Figure 5. The velocity at section A showed a skewness of flow towards the inner side of aorta. The angular neck bending induces fluid motion as shown at sections B and C. Therefore, the flow velocity near the wall of proximal and aneurysm aorta is forming C-shaped of velocity distribution directed towards the inner side of aorta at both sections B and C, respectively. It is also can be noticeable that the flow of blood is concentrated clearly near and around the aneurysm sac wall. For planes D, E and F, the velocity distributions suggest notable disturbances and significant increase up to 0.7 m/s at bifurcation area

and iliac arteries. This is occurred because of flow bifurcating together with the pressure gradient at iliac arteries [9].

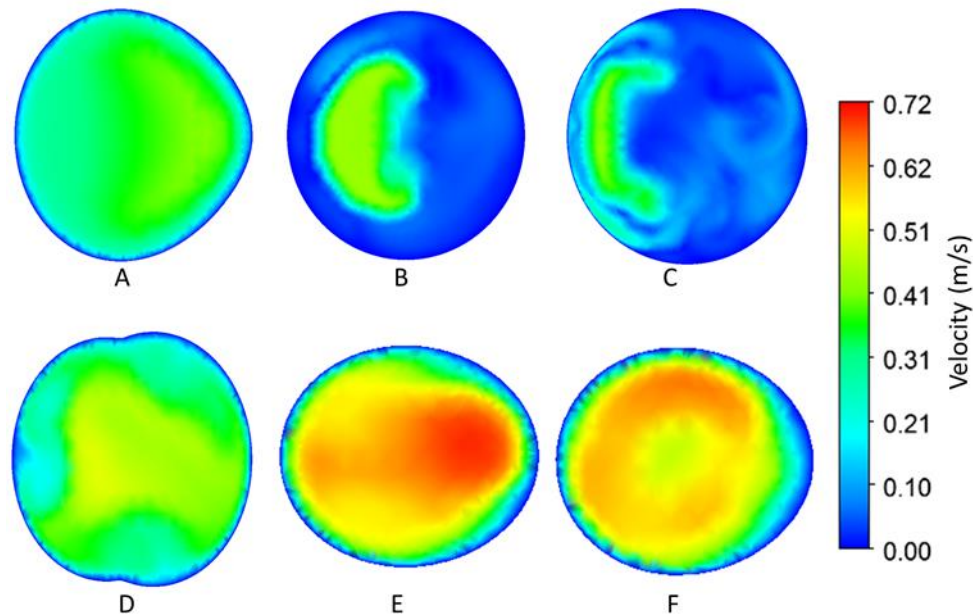


Fig. 5. Velocity profiles at selected planes for the steady state simulations

For the transient simulation, the dynamics of blood flow were investigated at two-time frames: maximum velocity ($t = 0.25$ s as peak systole) and minimum velocity ($t = 0.55$ s as early diastole). Figure 6 illustrates the velocity contours of pulsatile simulation results at the two time-points in a cardiac cycle. These time-frames were selected because they are considered as critical cardiac phases. The locations of cross-sectional planes can be referred to Figure 1. It is noticed that the blood flow in at systolic phase ($t = 0.25$ s) is increased during it flows downward to iliac arteries as presented in the planes. The velocity increases until maximum value of 0.72 m/s at the outlet regions which estimated to be approximately 50%. The reasons of the flow differences and the significant increase at regions (D, E and F) are influenced by the high pressure and anatomical structure of AAA model e.g. the aneurysm sac and arterial bifurcation. These results show an agreement with previous study by Algabri *et al.*, [25] and Soares *et al.*, [26]. On the other hand, the flow at a diastolic phase ($t = 0.55$ s) showed a distinct changed behavior from the flow at a systolic phase. These changes can be clearly seen three ways: the decrease of velocity magnitude to almost 25-30 %, the flow direction towards wall side and aneurysm sac (see sections B and C) and forming a circular-shaped of flow near the wall as seen in sections E and F. From Figure 5 and Figure 6 especially at regions of D, E and F, we can observe high velocity. This phenomenon shows a consistency with prior study of Liu *et al.*, [27], this can be caused by high pressure at these regions.

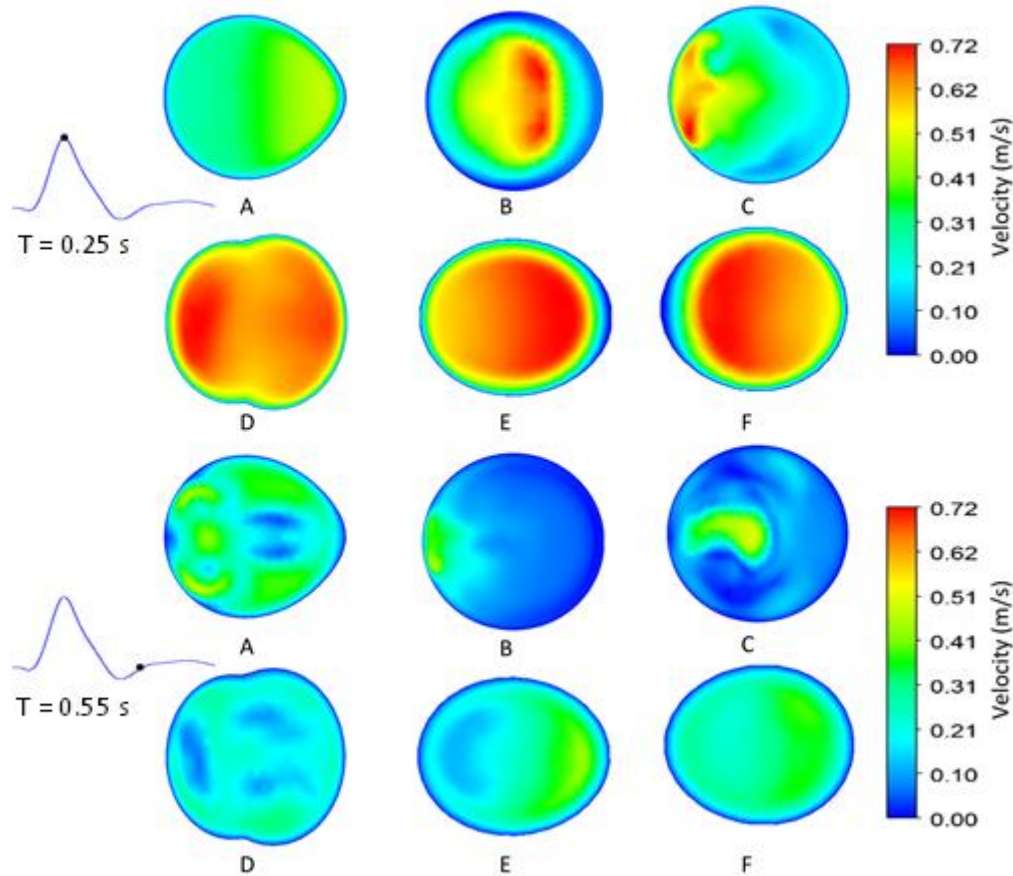


Fig. 6. Velocity profiles at cross-sectional planes for two time-frames

3.3. Flow Rate

The flow rate was calculated for both steady and transient flow at outlets of iliac arteries as presented in Figure 7. The flow rate (Q) was calculated based on Eq. (3) [23].

$$Q = v \cdot A \text{ (m}^3\text{/s)} \quad (3)$$

where v is velocity and A is the outlets area (Right and left iliac arteries). The graph illustrates the flow rate variance between steady and transient ($t = 0.25$ s and $t = 0.55$ s) flow conditions at both outlet of iliac arteries for a highly angulated neck of AAA model. It is noticed that high flow rate occurred at steady and transient ($t = 0.25$ s) states, this due to the maximum velocity imposed at inlet boundary. On other hand, flow rate seems to be less at diastolic phase ($t = 0.55$ s).

Furthermore, the flow rate for each outlet (right and left) of iliac arteries appears to be slightly different in both steady and transient flow conditions. However, it observed that the flow rate at left iliac appears to be higher than in right iliac outlet. This difference could be referred to the influence of proximal neck of AAA, anatomical curvature of model and pressure at these regions. It is proper to mention that a possible limitation might influence the study results such as assuming blood as Newtonian fluid. It is known that blood exhibits a non-Newtonian behavior. However, Newtonian assumption has been considered acceptable since minor differences in the basic flow characteristics are introduced through the non-Newtonian hypothesis [28].

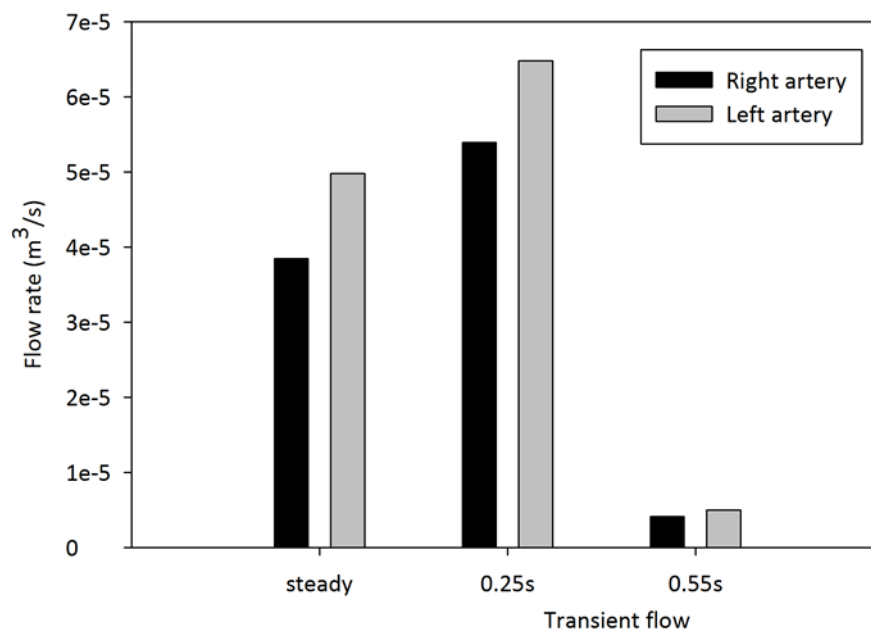


Fig. 7. Flow rate at both iliac artery outlets for steady and transient states

4. Conclusion

Computational fluid dynamics simulations for 3D idealized severe proximal neck of AAA model were performed based on patient hemodynamic parameters obtained from previous experimental study. The main aim of this work was to investigate and assess the differences between the steady and transient flow behaviours within proximal neck, aneurysm sac and iliac arteries for abdominal aortic aneurysm. In order to achieve this aim of study, CFD tools were adopted under the steady and transient simulations. High velocity was observed to be higher in the planes of D, E and F in both steady and transient models. In transient phase ($t = 0.25$ s), the velocity at outlets was increased up to 0.72 m/s and flow rate at the outlet of iliac arteries was higher compared with the steady condition. The investigated parameters have shown pronounced differences in the transient case more than in the steady case. The changes in velocity and flow pattern through the aneurysm and bifurcated arteries will be useful for the understanding of cardiovascular disease intervention.

Acknowledgement

This work was sponsored by the Thailand's Education Hub for Southern Region of ASEAN Countries (TEH-AC) scholarship from graduate school, Prince of Songkla University (Grant No: 009/2016).

Conflict of Interests

Authors declare that no conflict of interests in this study.

References

- [1] Tan, F. P. P., A. Borghi, R. H. Mohiaddin, N. B. Wood, S. Thom, and X. Y. Xu. "Analysis of flow patterns in a patient-specific thoracic aortic aneurysm model." *Computers & Structures* 87, no. 11-12 (2009): 680-690.
- [2] Joly, Florian, Gilles Soulez, Damien Garcia, Simon Lessard, and Claude Kauffmann. "Flow stagnation volume and abdominal aortic aneurysm growth: Insights from patient-specific computational flow dynamics of Lagrangian-coherent structures." *Computers in Biology and Medicine* 92 (2018): 98-109.
- [3] Sakalihasan, Natzi, Raymond Limet, and Olivier Damien Defawe. "Abdominal aortic aneurysm." *The Lancet* 365, no. 9470 (2005): 1577-1589.

- [4] Cecchi, Emanuele, Cristina Giglioli, Serafina Valente, Chiara Lazzeri, Gian Franco Gensini, Rosanna Abbate, and Lucia Mannini. "Role of hemodynamic shear stress in cardiovascular disease." *Atherosclerosis* 214, no. 2 (2011): 249-256.
- [5] Lozowy, Richard J., David CS Kuhn, Annie A. Ducas, and April J. Boyd. "The relationship between pulsatile flow impingement and intraluminal thrombus deposition in abdominal aortic aneurysms." *Cardiovascular Engineering and Technology* 8, no. 1 (2017): 57-69.
- [6] Biehler, Jonas, Sebastian Kehl, Michael W. Gee, Fadwa Schmies, Jaroslav Pelisek, Andreas Maier, Christian Reeps, Hans-Henning Eckstein, and Wolfgang A. Wall. "Probabilistic noninvasive prediction of wall properties of abdominal aortic aneurysms using Bayesian regression." *Biomechanics and Modeling in Mechanobiology* 16, no. 1 (2017): 45-61.
- [7] Argani, L. P., F. Torella, R. K. Fisher, R. G. McWilliams, M. L. Wall, and A. B. Movchan. "Deformation and dynamic response of abdominal aortic aneurysm sealing." *Scientific Reports* 7, no. 1 (2017): 17712.
- [8] Peattie, Robert A., Tiffany J. Riehle, and Edward I. Bluth. "Pulsatile flow in fusiform models of abdominal aortic aneurysms: flow fields, velocity patterns and flow-induced wall stresses." *Journal of Biomechanical Engineering* 126, no. 4 (2004): 438-446.
- [9] Vasava Paritosh, Payman Jalali, Mahsa Dabagh, and Pertti J. Kolari. "Finite element modelling of pulsatile blood flow in idealized model of human aortic arch: study of hypotension and hypertension." *Computational and Mathematical Methods in Medicine* 2012 (2012).
- [10] Dabagh Mahsa, Payman Jalali, Yrjö T. Konttinen, and Pertti Sarkomaa. "Distribution of shear stress over smooth muscle cells in deformable arterial wall." *Medical & Biological Engineering & Computing* 46, no. 7 (2008): 649-657.
- [11] Towfiq, B. A., J. Weir, and J. M. Rawles. "Effect of age and blood pressure on aortic size and stroke distance." *Heart* 55, no. 6 (1986): 560-568.
- [12] Bluestein, Danny. "Utilizing Computational Fluid Dynamics in cardiovascular engineering and medicine—What you need to know. Its translation to the clinic/bedside." *Artificial organs* 41, no. 2 (2017): 117-121.
- [13] Noh, Arina Mohd, Sohif Mat, and Mohd Hafidz Ruslan. "CFD Simulation of Temperature and Air Flow Distribution inside Industrial Scale Solar Dryer." *Journal of Advanced Research in Fluid Mechanics and Thermal Sciences* 45, no. 1 (2018): 156-164.
- [14] Carty, Gregory, Surapong Chatpun, and Daniel M. Espino. "Modeling blood flow through intracranial aneurysms: A comparison of Newtonian and non-Newtonian viscosity." *Journal of Medical and Biological Engineering* 36, no. 3 (2016): 396-409.
- [15] Miyazaki, Shohei, Keiichi Itatani, Toyoki Furusawa, Teruyasu Nishino, Masataka Sugiyama, Yasuo Takehara, and Satoshi Yasukochi. "Validation of numerical simulation methods in aortic arch using 4D Flow MRI." *Heart and Vessels* 32, no. 8 (2017): 1032-1044.
- [16] Jaat, Norrizam, Amir Khalid, Norrizal Mustaffa, Fathul Hakim Zulkifli, Norshuhaila Mohamed, Ridwan Saputra Nursal Sunar, Mahmud Abd Hakim Mohamad, and Djamel Didane. "Analysis of Injection Pressure and High Ambient Density of Biodiesel Spray using Computational Fluid Dynamics." *CFD Letters* 11, no. 1 (2019): 28-39.
- [17] Morrison, Tina M., Clark A. Meyer, Mark F. Fillinger, Ron M. Fairman, Marc H. Glickman, Richard P. Cambria, Mark A. Farber, *et al.*, "Eligibility for Endovascular Repair of Short Neck Abdominal Aortic Aneurysms." *Journal of Vascular Surgery* 57, no. 5 (2013): 24S.
- [18] Xenos, Michalis, Yared Alemu, Dan Zamfir, Shmuel Einav, John J. Ricotta, Nicos Labropoulos, Apostolos Tassiopoulos, and Danny Bluestein. "The Effect of Angulation in Abdominal Aortic Aneurysms: Fluid-Structure Interaction Simulations of Idealized Geometries." *Medical and Biological Engineering and Computing* 48, no. 12 (December 19, 2010): 1175–90.
- [19] Yeow, Siang Lin, and Hwa Liang Leo. "Hemodynamic Study of Flow Remodeling Stent Graft for the Treatment of Highly Angulated Abdominal Aortic Aneurysm." *Computational and Mathematical Methods in Medicine* 2016 (May 9, 2016): 1–10.
- [20] Ku, David N. "BLOOD FLOW IN ARTERIES." *Annual Review of Fluid Mechanics* 29, no. 1 (1997): 399–434.
- [21] Hobo, Roel, Jur Kievit, Lina J. Leurs, and Jacob Buth. "Influence of severe infrarenal aortic neck angulation on complications at the proximal neck following endovascular AAA repair: a EUROSTAR study." *Journal of Endovascular Therapy* 14, no. 1 (2007): 1-11.
- [22] Clement Ajani, Stefano Curcio, Racha Dejchanchaiwong, and Perapong Tekasakul. "Influence of shrinkage during natural rubber sheet drying: Numerical modeling of heat and mass transfer." *Applied Thermal Engineering* 149 (2019): 798-806.
- [23] Algabri, Y. A., S. Rookkapan, and S. Chatpun. "Three-dimensional finite volume modelling of blood flow in simulated angular neck abdominal aortic aneurysm." In *IOP Conference Series: Materials Science and Engineering*, vol. 243, no. 1, p. 012003. IOP Publishing, 2017.

-
- [24] Olufsen, Mette S., Charles S. Peskin, Won Yong Kim, Erik M. Pedersen, Ali Nadim, and Jesper Larsen. "Numerical simulation and experimental validation of blood flow in arteries with structured-tree outflow conditions." *Annals of Biomedical Engineering* 28, no. 11 (2000): 1281-1299.
- [25] Algabri, Yousif A, Sorracha Rookkapan, Vera Gramigna, Daniel M Espino, and Surapong Chatpun. "Computational Study on Hemodynamic Changes in Patient-Specific Proximal Neck Angulation of Abdominal Aortic Aneurysm with Time-Varying Velocity." *Australasian Physical & Engineering Sciences in Medicine* 42, no. 1 (2019): 181–190.
- [26] Soares, Armando A., Sílvia Gonzaga, Carlos Oliveira, André Simões, and Abel I. Rouboa. "Computational fluid dynamics in abdominal aorta bifurcation: non-Newtonian versus Newtonian blood flow in a real case study." *Computer methods in Biomechanics and Biomedical Engineering* 20, no. 8 (2017): 822-831.
- [27] Liu, Ming, Anqiang Sun, and Xiaoyan Deng. "Hemodynamic performance within crossed stent grafts: computational and experimental study on the effect of cross position and angle." *BioMedical Engineering OnLine* 17, no. 1 (2018): 85.
- [28] Perktold, K., M. Resch, and H. Florian. "Pulsatile non-Newtonian flow characteristics in a three-dimensional human carotid bifurcation model." *Journal of Biomechanical Engineering* 113, no. 4 (1991): 464-475.